MECSOL 2019 - Proceedings of the 7th International Symposium on Solid Mechanics,
Angelo, M. V.; Ribeiro, M. L.; Madureira, F.; Tita, V., ABCM, Sao Carlos, SP, Brazil, April 15th to 17th, 2019

Onset and Crack Propagation of Composite Structures: Numerical and Experimental Analyses

Angelo, M. V.; Ribeiro, M. L.; Madureira, F.; Tita, V.

Universidade de São Paulo, Av. João Dagnone, 1100 - Jardim Santa Angelina – São Carlos – SP - Brazil

In order to proper evaluate mechanical behavior of tapered composite structures a new framework of analysis is proposed based on the theory of failure by Alfred Puck, implemented on an 3D XFEM routine. A new optimization algorithm is proposed in order to determine the initial onset crack angle. After extensive validation against literature results and experiments built specifically for capturing the mechanisms of interest, the model was found to be robust, capable of correctly reproducing ultimate load and more than 20 times more efficient than current implementations.

Keywords: 3D XFEM, crack propagation, tapered structures

INTRODUCTION

Even with all the progress achieved through fracture mechanics and damage theory, the field of failure onset and propagation on complex composite structures is wide open and of special interest for high performance industries such as automotive and aerospace.

Latter approaches involving fracture mechanics and RVEs (Representative Volume Elements) are still steps away from being totally applicable at industry level which leads to the preference outside academic field for simpler, phenomenological models that present themselves both computational efficient and relatively robust. Among these models, the one developed by Puck and Schürmann (1998; 2002) is to be highlighted by its extensive usage in aeronautical industry. This may be explained by its excellent results in Worldwide Failure Exercise I and II, which stated "exhibiting good predictive capability, none or one fundamental weakness and many relatively minor weaknesses" (Hinton *et al.*, 2002; Kaddour *et al.*, 2004; Soden *et al.*, 2004).

The present work presents a new computational framework to evaluate composite structures by enhancing original Puck's method with a new optimization approach to define the angle at which failure occurs. This information is than used to trigger an XFEM routine that computes and enriches the elements according to the model definition. Tapered composite structures are used in aeronautical industry in many components including vital parts such as the main rotor hub on rotorcraft (Figure 1).

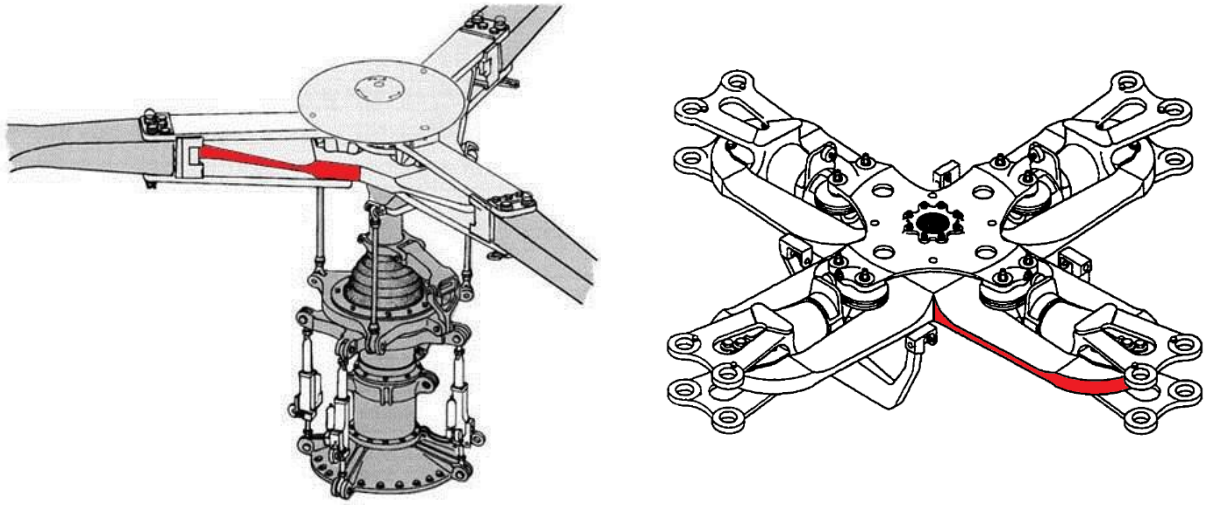

Figure 1 – Helicopter rotor hub, example of tapered structure (Lalonde, 2000)

The structures presented in Figure 1 are responsible for holding the blades and thus they shall withstand all the centrifugal efforts that will apply and, due to the cyclic efforts, they must hold the bending forces at each rotation.

METHODS

To proper reproduce mechanical behavior of a tapered structure both in plane and out of plane stress must be well computed. In the present work fiber and matrix mechanisms are treated isolated.

Matrix mechanisms

According to Pucks theory, in order to quantify matrix failure, a new coordinate system is defined at each mesh integration point. By averaging the stress tensor in the new orientation system, a failure index is calculated according to Eq. (1) and used to quantify the amount of damage in the matrix at each integration point measured on the action plane. This index will be argument for the determination of the damage variable for inter-fiber mechanism as in Eq. (2). Mechanical property will be degraded by this amount following Eq. (3).

$$IFF_A = \sqrt{\left[\left(\frac{1}{Y^t} - \frac{p_{\perp\parallel}^{t\,*}}{S_{12}}\right)\sigma_{22}\right]^2 + \left(\frac{\sigma_{12}}{S_{12}}\right)^2} + \frac{p_{\perp\parallel}^{t\,*}}{S_{12}}\sigma_{22} \tag{1}$$

$$\eta_{E/G} = \frac{1 - \eta_r^{E/G\,*}}{1 + c^*{}_{E/G}(IFF_A - 1)^{\xi^*_{E/G}}} + \eta_r^{E/G\,*} \tag{2}$$

$$E_{22} = \eta_E\, E_{22} \qquad\qquad G_{12} = \eta_G\, G_{12} \tag{3}$$

Y^t	Ultimate stress on fiber transversal direction
S_{12}	Ultimate shear stress on 1-2 direction
$p_{\perp\parallel}^t$	Puck's angular parameter
$\eta_r^{E/G\,*}$	Damage variable for the matrix
$c_{E/G}$	Puck's "c" parameter – measure on transversal direction and shear
$\xi_{E/G}$	Puck's ξ parameter – measure on transversal direction and shear
σ_{ab}	Stress on direction a-b

One point to be considered on implementing Puck's theory is the proper identification of the so-called action plane. This is the direction in which the stress index, according to the criterion, takes the maximum value. Figure 2 presents how the failure index evolves with respect to the inclination of action plane. In its original presentation, this plane was proposed to be found by brute force, i.e. every possible angle is swept and among the calculation of failure index for each of them the maximum value is chosen and used to determine action plane inclination, which is perfect for avoiding the local maxima but is extremely inefficient in terms of computational cost.

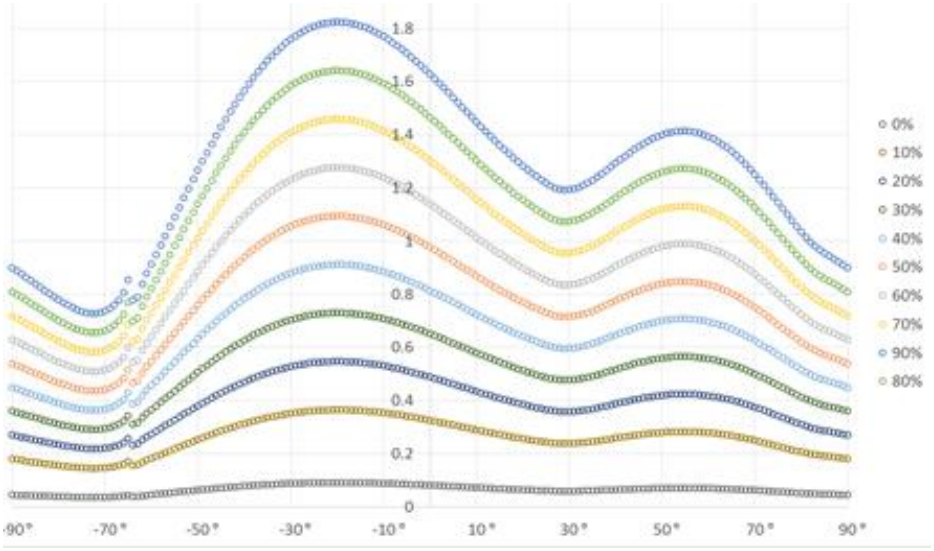

Figure 2 – Example of calculation of action plane inclination as proposed by Puck's Theory

To overcome this limitation a new method is proposed in which the Golden Section algorithm for optimization is applied piecewise over the interval [90°,-90°]. In each of nine 20° subinterval the algorithm is applied and the maximum failure index is determined by comparing values obtained in each subinterval. Assuming the hypothesis of Schirmaier et al. (2014) that there are no local maxima within 25° distance from each other, the subdivision is important to make sure that every local extremum is avoided and the model could find indeed the global maximum. The interval of interest, in this case [-90,90], was subdivided as per the golden ratio shown in Eq. (4):

$$\varphi = \frac{1+\sqrt{5}}{2} \tag{4}$$

Table 1 shows the performance enhancement achieved with the new approach taking as reference classic Puck with 1° step of sweep.

Table 1 – Performance comparison.

Approach	Precision Level		
	1.0º	0.5º	0.1º
Puck (reference)	**1.000**	2.000	10.00
Golden Section	0.061	0.072	0.089
Enhanced Golden Section	0.550	0.650	0.444

Fiber mechanisms

For fiber failure, the brittle and abrupt character is treated with a non-local approach. For each integration point in the mesh, a characteristic neighborhood is defined due to a non-local criterion (Miot *et al.*, 2010; Hochard *et al.*, 2014). It contains the set, herein named Characteristic Volume of Rupture (CVR) of integration points within a distance of the Characteristic Radius (CR) Figure 3.

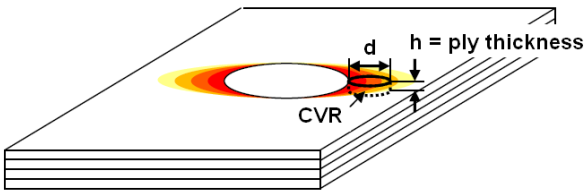

Figure 3 – The Characteristic Volume of Rupture and Characteristic Radius

The value of the CR is a material characteristic and may be obtained from elementary tests with stress concentrator presence. At each step, the model performs a sweep throughout an application zone in the structure and, for each point,

calculates a weighted average of the current longitudinal strain within the region bounded by each set as displayed by Eq. (5).

$$\overline{\varepsilon_{11}} = \frac{\sum^{i} \varepsilon_{11}^{i} V^{i}}{\sum^{i} V^{i}} \tag{5}$$

This procedure intends to minimize concentration, which may affect the convergence during the calculus and it is a space criterion to control high strain rates and gradients. The average strain is passed as argument along with mechanical ultimate longitudinal strain to Eq. (6), which calculates the longitudinal damage variable to be used for updating E_{11}:

$$\omega = 1 - \exp\left(-\frac{1}{m_{t/c}^{*} e_{t/c}^{*}}\left(\frac{\varepsilon_{11}}{\varepsilon_{t/c}^{f}}\right)^{m_{t/c}^{*}}\right) \tag{6}$$

The longitudinal damage variable is then used to upgrade the material property E11. Therefore, the Eq. (7) shows the degradation of the property due to fiber failure:

$$E_{11} = \omega\, E_{11}^{0} \tag{7}$$

RESULTS

The proposed approach was implemented into Abaqus subroutines UMAT-UDMGINI-URDFIL. Two types of tests were performed to validate the model: compact tension and tapered and for each type, two different stack sequence were considered

Compact tension

Ten specimens were manufactured according to the geometry presented in Figure 4

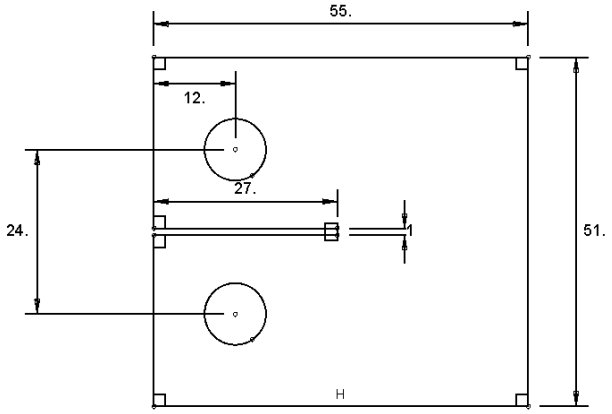

Figure 4 – The Characteristic Volume of Rupture and Characteristic Radius

Five parts were manufactured at each of the following stacking sequences:

A – 5 specimens with 37 layers -> [[0,90]9,0,[90,0]9]

B – 5 specimens with 33 layers -> [[0,45,90,-45]4,0,[-45,90,45,0]4].

The setup of the test may be seen on Figure 5.

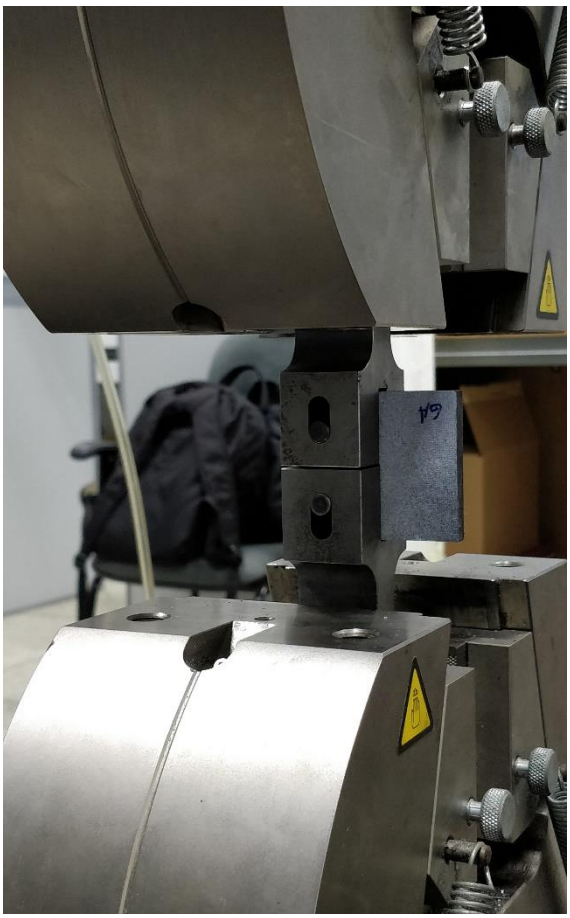

Figure 5 – Setup for compact tension test

By means of image correlation, it was possible to monitor the strain during the test. The results for each stack sequence may be found on Figure 6, where it is plotted the reaction force of the structure versus the displacement applied.

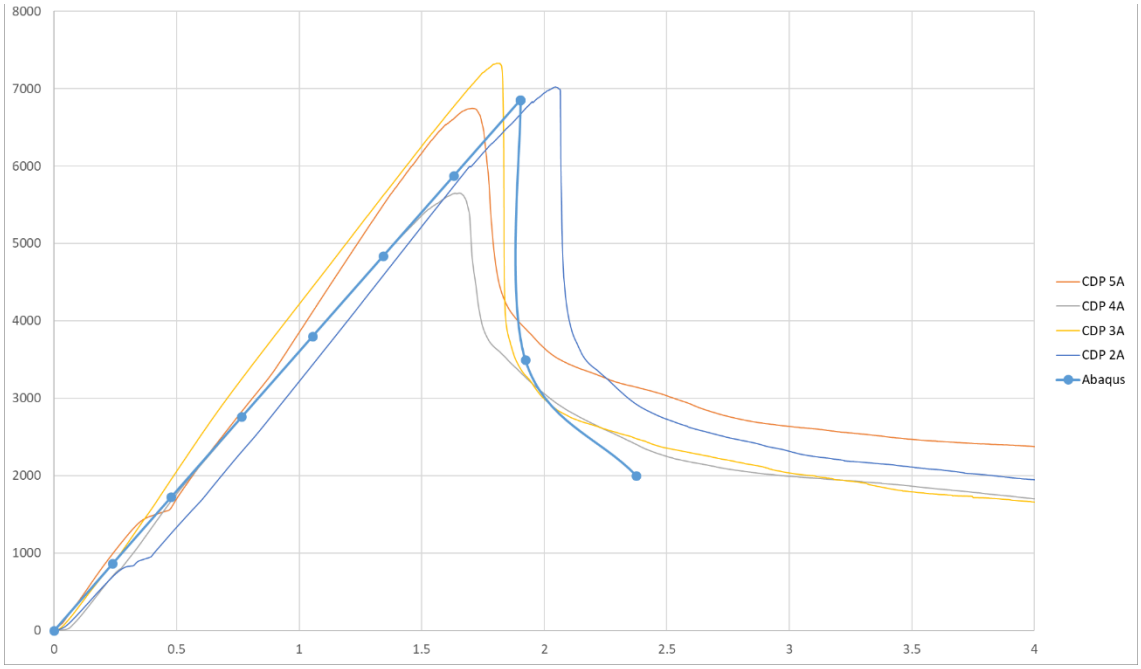

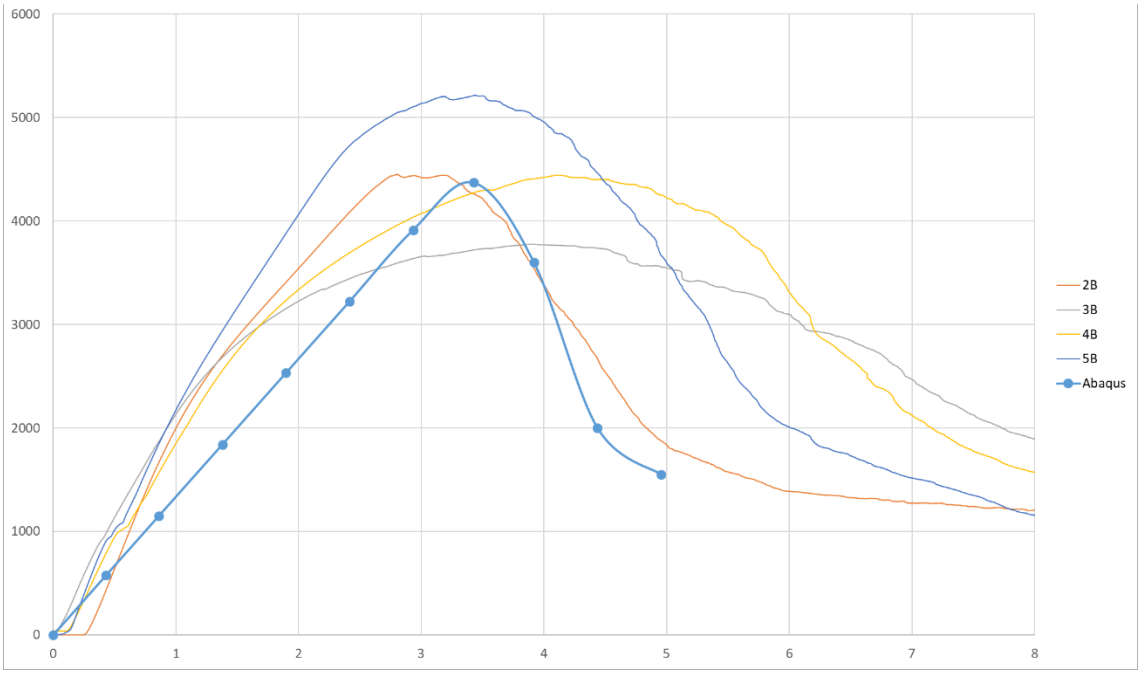

Figure 6 – Load [N] vs Displacement [mm] for the compact tension specimens (A) and (B)

A comprehensive summary of the results is presented on Table 2.

Table 2 – Performance comparison.

Specimen	Ultimate load (N)	Model	Specimen	Ultimate load (N)	Model
5A	5215.82	4371.09	5B	6745.32	6745.32
4A	4443.94		4B	5652.69	
3A	3777.76		3B	7327.33	
2A	4453.19		2B	7022.71	
Mean	4472.67	-	Mean	6687.01	-
Std deviation	587.76	-	Std deviation	729.36	-

Tapered structure

To evaluate the performance of the model when applied to the final structure it was developed for, 6 specimens were manufactured according to the geometry displayed in Figure 7.

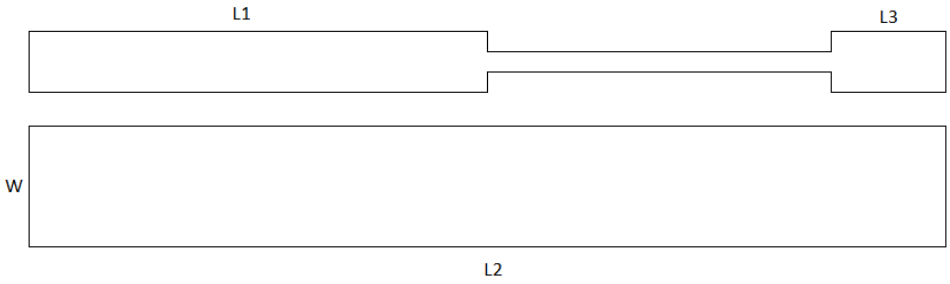

Figure 7 – Geometry of tapered specimens

The six specimens were divided in two different stack sequences. The dimensions for each stacking sequence are shown in Table 3.

Table 3 – Dimensions of tapered specimen

CDP	L1 (mm)	L2 (mm)	L3 (mm)	W (mm)	Stack
A	80	160	30	30	$[0,45,90,-45,0,-45,90,45,0]_3$
B	80	160	30	11	$[[0]_2,[90]_5,[0]_2]_3$

The test setup for the tapered experiments may be found in Figure 8.

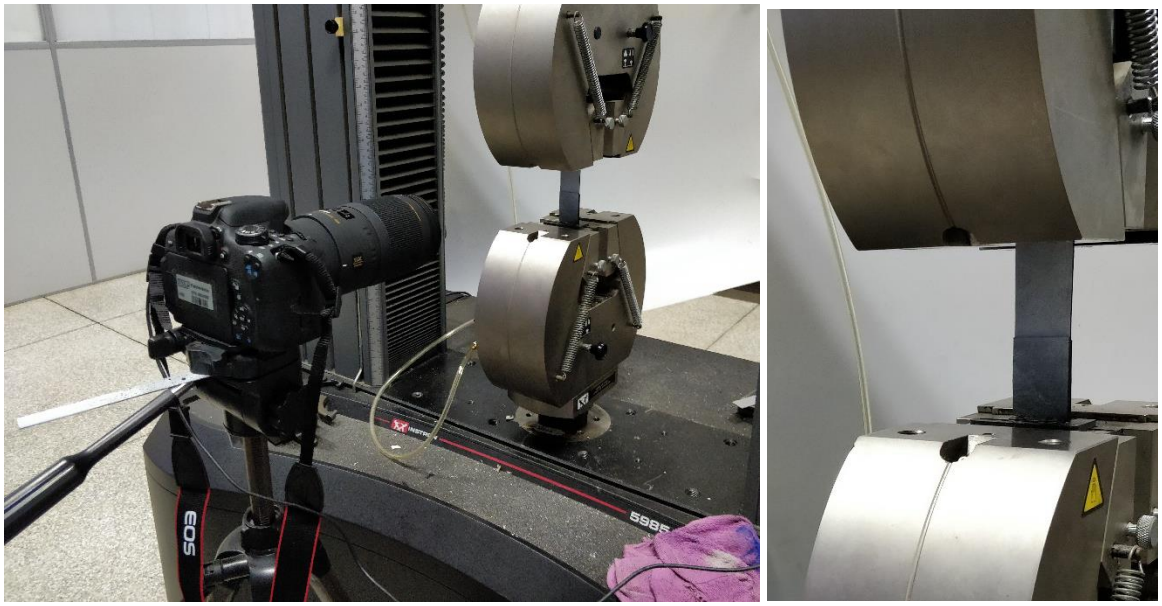

Figure 8 – Setup of experiment for tapered specimens

The tests were displacement imposed and strain was monitored through image correlation. Figure 9 shows the result comparison for strain versus load for the specimens “A”.

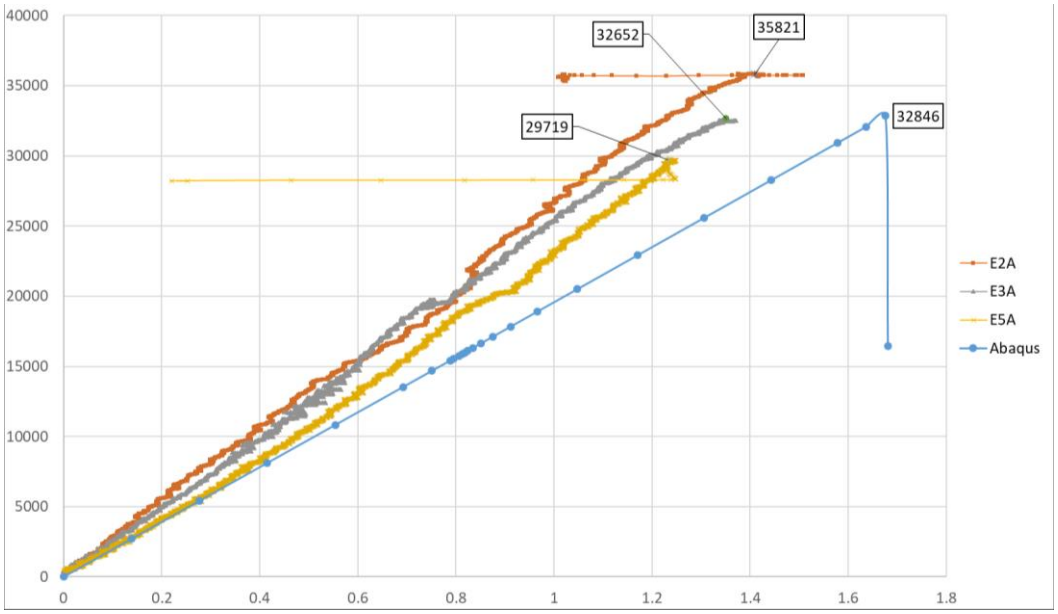

Figure 9 – Load [N] vs Strain for specimens “A”

The strain values were obtained by a virtual strain gage placed 10mm from the ply drop at the center line of the specimen. Table 4 shows the numerical comparison for the results.

Table 4 – Comparison of results obtained for specimen "A"

Specimen	Ultimate Load (N)	Model	Maximum strain	Model
E5A	29718.9	32846.1	1.232	1.676
E3A	32651.8		1.352	
E2A	35821.1		1.409	
Mean	32730.6	-	1.331	-
Std deviation	3051.8	-	0.090	-

Analogously, the same analysis is presented for specimens "B". Figure 10 shows the results for the three specimens with this stacking sequence.

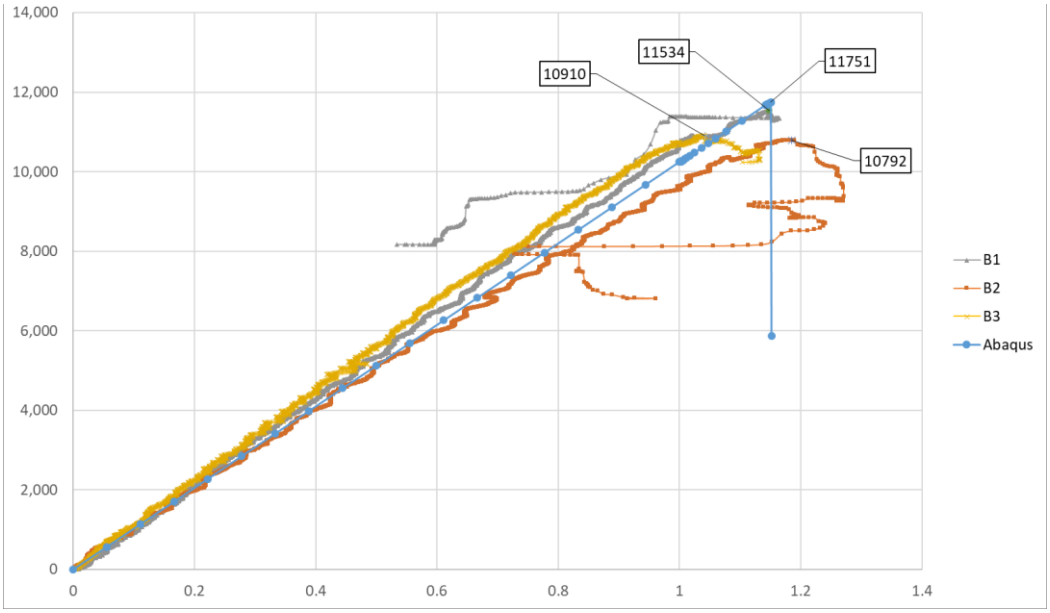

Figure 10 – Load [N] vs Strain for specimens "B"

Table 5 shows the numerical comparison between the results obtained from the model and from the experiments.

Table 5 – Comparison of results obtained for specimen "B"

Specimen	Ultimate Load [N]	Model	Maximum Strain	Model
B1	11533.9	11751.2	1.148	1.151
B2	10791.6		1.185	
B3	10909.6		1.041	
Meana	11078.4	-	1.125	-
Std Deviation	398.9	-	0.075	-

CONCLUSION

The present work showed a new framework, combining XFEM and 3D Puck's failure theory, for evaluating onset and propagation of failure (evolution of cracks) on tapered composite structures.

Besides, the proposed approach for determining crack inclination angle has proven to be robust and precise, filling a gap on the available researches in the field. Compared to the algorithm proposed by Puck, the new methodology has convergence one order higher than the first method developed by Puck; it is 20 times more efficient computationally for a 0.1° precision. Therefore, if more precision is needed, then higher gains are achieved by using the proposed method. Simple tests were simulated both in tension and compression, displaying results as expected.

REFERENCES

HINTON, M. J.; KADDOUR, A. S.; SODEN, P. D. A Comparison of the Predictive Capabilities of Current Failure Theories for Composite Laminates, Judged Against Experimental Evidence. **Composites Science and Technology,** v. 62, n. 12, p. 1725-1797, 2002. ISSN 0266-3538. Disponível em: < http://doi.org/10.1016/S0266-3538(02)00125-2 >.

HOCHARD, C.; MIOT, S.; THOLLON, Y. Fatigue of laminated composite structures with stress concentrations. **Composites Part B: Engineering,** v. 65, p. 11-16, 2014/10/01/ 2014. ISSN 1359-8368. Disponível em: < http://www.sciencedirect.com/science/article/pii/S1359836813005957 >.

KADDOUR, A. S.; HINTON, M. J.; SODEN, P. D. A Comparison of the Predictive Capabilities of Current Failure Theories for Composite Laminates: Additional Contributions. **Composites Science and Technology,** v. 64, n. 3, p. 449-476, 2004. ISSN 0266-3538. Disponível em: < http://doi.org/10.1016/S0266-3538(03)00226-4 >.

LALONDE, S. **Investigation Into The Static and Fatigue Bedaviour of a Helicopter Main Rotor Yoke Made of Composite Materials**. 2000. 92 (Master of Engineering). Department of Mechanical Engineering, McGill University, Ottawa.

MIOT, S.; HOCHARD, C.; LAHELLEC, N. A Non-Local Criterion for Modelling Unbalanced Woven Ply Laminates with Stress Concentrations. **Composite Structures,** v. 92, n. 7, p. 1574-1580, 2010. ISSN 0263-8223. Disponível em: < http://doi.org/10.1016/j.compstruct.2009.11.019 >.

PUCK, A.; SCHÜRMANN, H. Failure Analysis of FRP Laminates by Means of Physically Based Phenomenological Models. **Composites Science and Technology,** v. 58, n. 7, p. 1045-1067, 1998. ISSN 0266-3538. Disponível em: < http://doi.org/10.1016/S0266-3538(96)00140-6 >.

_____. Failure Analysis of FRP Laminates by Means of Physically Based Phenomenological Models. **Composites Science and Technology,** v. 62, n. 12, p. 1633-1662, 2002. ISSN 0266-3538. Disponível em: < http://doi.org/10.1016/S0266-3538(01)00208-1 >.

SCHIRMAIER, F. J. et al. A New Efficient and Reliable Algorithm to Determine the Fracture Angle for Puck's 3D Matrix Failure Criterion for UD Composites. **Composites Science and Technology,** v. 100, p. 19-25, 2014. ISSN 0266-3538. Disponível em: < http://dx.doi.org/10.1016/j.compscitech.2014.05.033 >.

SODEN, P. D.; KADDOUR, A. S.; HINTON, M. J. Recommendations for Designers and Researchers Resulting from the World-Wide Failure Exercise. **Composites Science and Technology,** v. 64, n. 3–4, p. 589-604, 2004. ISSN 0266-3538. Disponível em: < http://dx.doi.org/10.1016/S0266-3538(03)00228-8 >.

RESPONSIBILITY NOTICE

The author(s) is (are) the only responsible for the printed material included in this paper.